# Marwan2

*by* Marwan2 Marwan2

**Submission date:** 25-Jul-2023 12:52PM (UTC+0700)
**Submission ID:** 2136480409
**File name:** BCWSP50066.2020.9249448.pdf (544.81K)
**Word count:** 4349
**Character count:** 21298

# A Study on Modular Multilevel Converter based Wind Turbine Generator Connected to Medium Voltage DC Collection Network


Marwan Rosyadi
*Dept. of School of Earth, Energy and Environmental Eng*
*Kitami Institute of Technology*
Kitami, Japan
marwanrosyadi@gmail.com

Atsushi Umemura
*Dept of School of Earth, Energy and Environmental Eng.*
*Kitami Institute of Technology*
Kitami, Japan
umemura@mail.kitami-it.ac.jp

Rion Takahashi
*Dept. of School of Earth, Energy and Environmental Eng.*
*Kitami Institute of Technology*
Kitami, Japan
rtaka@mail.kitami-it.ac.jp

Junji Tamura
*Dept. of School of Earth, Energy and Environmental Eng.*
*Kitami Institute of Technology*
Kitami, Japan
tamuraj@mail.kitami-it.ac.jp



***Abstract*— This study proposes an application of Modular Multilevel Converter (MMC) to wind turbine direct driven Permanent Magnet Generator (PMG) which is connected to medium voltage DC collection network. The topology, modeling, operation, and control method of the wind turbine generator connected to MMC system are presented. The aim of the application of MMC to the wind turbine generator is to increase its operating voltage so as to be connected to medium voltage of DC network. Besides that, a grid side converter, a harmonic filter device and a transformer of the wind turbine generator can be neglected. Feasibility and validity of operation and control method of the proposed MMC based wind turbine generator have been investigated through simulation study. The simulation is performed by using PSCAD/ EMTDC package program. The obtained results have confirmed that the proposed topology and control system have good dynamic performance, controllability, and reliable stability.**



***Keywords— modular multilevel converter, permanent magnet generator, DC collection network, wind farm.***


## I. INTRODUCTION

Wind turbine generators based offshore power stations are predicted to be growing rapidly along with the increasing world demand to meet energy needs, especially from renewable energy resources. The potential energy which can be generated from offshore wind is more than 420.000 TWh per year worldwide, and hence, in the future, offshore wind farm would have a big influence on the global energy market [1]. The development of offshore wind is resulting from the developing technology of wind turbine generators and their grid connected devices of variety of power capacity which in turn can provide cost improvements and high performances for offshore wind farm.

The possibility for the use of DC collection network systems in offshore wind farms has been widely reported in several papers [1-5]. Many advantages in using a DC network system in offshore over AC networks are obtained, i.e., no system stability issues, fast adjustment and reliable operation, no capacitor charging current and limited short-circuit current, high efficiency, low channel cost due to weight and material savings, small annual energy loss, etc. However, the benefits of using a DC network system will be optimized if operated on a medium and high voltage network.

In the DC network system converter devices should be included. LCC (Line Commutated Converter and VSC (Voltage Source Converter) are converter technology commonly used in DC network. MCC is a latest generation of multi-level converter technology which is applied to HVDC system. In 2010, the first technology of MMC called HVDC PLUS has been introduced by Siemens [6]. In the same year ABB also commissioned the HVDC Light using same technology [7]. Nowadays, MMC is an innovative technology that has many advantages compared to other multilevel converter technologies such as Cascaded H-Bridges, Neutral Point Clamped Converter, and Flying-Capacitor Converter. MMC has a simpler structure, scalable and flexible design so that the expansion of the number of levels can be possible easily and the maintenance is also easy because submodules can be replaced easily [6-9].

In this paper, a feasibility of application of MMC for medium voltage class of wind turbine direct driven PMG is discussed. The application of AC to DC MMC to wind turbine generator is intended to eliminate its converter connected to grid side, harmonic filter device, and the transformer, and hence, the power production from wind generator can be collected through medium voltage of DC collection network. In addition, by using medium voltage operation the level of power capacity of wind turbine generator can be increased with light and smaller outer diameter of the generator due to reducing of the coil diameter of stator winding of the generator. The advantages possessed by MMC can be possible in its application to wind turbine generator which can operate with being connected to a medium voltage network. Therefore, investment costs of wind turbine generator based offshore wind farm can be reduced.

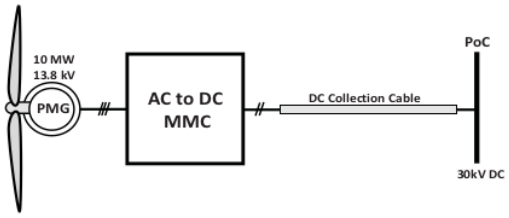


Fig. 1. Electrical topology of MMC based PMG


978-1-7281-7450-1/20/$31.00 ©2020 IEEE

## II. MMC BASED PMG

Fig. 1 depicts the electrical topology of the gearless wind turbine equipped with the AC to DC MMC system. Gearless system is a wind turbine generator system that drives generator directly without gearbox transmission system. The generator is Permanent Magnet Generator (PMG) which is equipped with multi-pole permanent magnet mounted on the rotor shaft. Three phases stator winding of the generator is connected to AC side of MMC. On the other hand, DC side of MMC is connected to 30 kV Point of Connection (PoC) network through DC collection power cable of 3.0 km. The DC collection cable is assumed here as collection network in an offshore wind farm.

### A. Modeling of Wind Turbine

The power of wind energy captured by the turbine can be calculated through equations as follows [10]:

$$P_{wt} = \frac{1}{2}\rho\,\pi\,R_b^2\,V_w^3\,C_p \tag{1}$$

where, $P_{wt}$ is mechanical power of wind turbine in W; $\rho$ *is* density of air in Kg/m$^3$; $R_b$ is blade radius of rotor in m; $V_w$ is wind velocity in m/s; and $C_p$ is the turbine power coefficient.

The power coefficient ($C_p$) of wind turbine is determined depending on tip speed ratio ($\lambda$) and pitch angle ($\beta$) of wind turbine's blades in degree. The turbine power coefficient can be expressed as follows:

$$C_p = c_{o1}\left(\frac{c_{o2}}{\lambda_i} - c_{o3}\beta - c_{o4}\right)e^{\frac{-c_{o5}}{\lambda_i}} + c_{o6}\lambda \tag{2}$$

$$\lambda = \frac{\omega_r R_b}{V_w} \tag{3}$$

$$\frac{1}{\lambda_i} = \frac{1}{\lambda - 0.08\beta} - \frac{0.035}{\beta^3 + 1} \tag{4}$$

where, $c_{O1}$ to $c_{O6}$ are the wind turbine's coefficients [11], and $\omega_r$ is speed of the wind turbine's rotor in rad/sec.

The Characteristic curve of $C_p$-$\lambda$ with different pitch angles is depicted in Fig. 2 from which it can be seen the maximum power coefficient ($C_{p\text{-}max}$) is 0.48 and the optimal tip speed ratio ($\lambda_{opt}$) is 8.1. Power output curve of the wind turbine as function of rotational speed is depicted in Fig. 3. In the direct drive wind turbine generator, the Maximum Power Point Trajectory ($P_{mppt}$) shown by the blue line can be calculated as follows [12]:

$$P_{mppt} = 0.5\rho\pi R^2\left(\frac{\omega_r R}{\lambda_{opt}}\right)^3 C_{p\text{-}max} \tag{5}$$

Rotating mass components of wind turbine generator are composed of rotor shaft including the magnet of generator, hub, and blades. The rotating mass components can be modelled in one lump or two lump models for analyzing dynamic behavior of the wind turbine under variation wind speed. In this paper one lump model is considered which could be expressed through the following equation [13]:

$$T_m - T_e = \frac{1}{J_t}\frac{d\omega_r}{dt} \tag{6}$$

The one lump model of the rotating mass is depicted in Fig. 4. $J_t$ represents total moment of inertia. $T_m$ and $T_e$ represents mechanical and electrical torques, respectively.

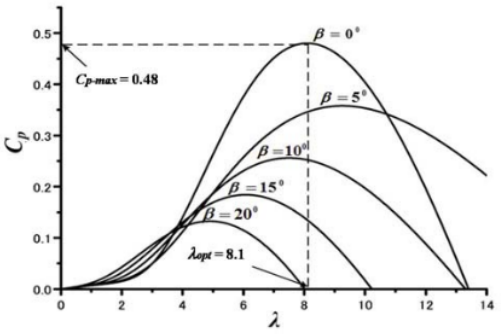


Fig. 2. Characteristic curve of Cp - $\lambda$

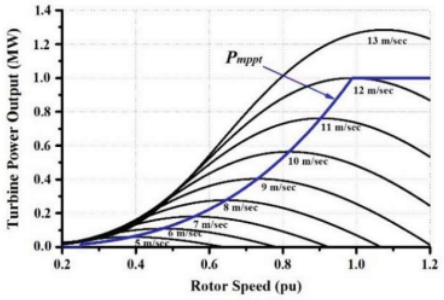


Fig. 3. Power curve of wind turbine ($\beta$=0$^0$)

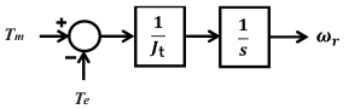


Fig. 4. One lump model of wind turbine's rotating mass

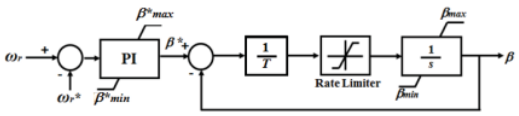


Fig. 5. Pitch blades control model

Pitch controller is very important in adjusting the angle attack ($\beta$) of the wind turbine's blades when the rotor speed of wind turbine exceeds its maximum speed. In general, the maximum speed of variable speed wind turbine is up to 30 rpm. In this paper, model of pitch blades controller is shown in Fig. 5, where, $\omega$* is rotational speed reference and $\beta$* is pitch angle reference. Each blade of the wind turbine is driven by a motor servo actuator which represented by transfer function with time constant $T$ and rate limiter. The ranges ($\beta_{min}$ to $\beta_{max}$) of pitch angle of blades is set from 0$^o$ to 90$^o$. The PI controller is commonly used for tracking error in the pitch controller system [13], [14].

### B. Permanent Magnet Generator (PMG)

The model of PMG used in this paper is based on available model in library of PSCAD/EMTDC software package [15]. The PMG model is represented in the d-q model equations which can be written as follows [16]:

$$V_d = RI_d + L_d\frac{dI_d}{dt} - \omega_s L_q I_q \quad (7)$$

$$V_q = RI_q + L_q\frac{dI_s}{dt} + \omega_s L_d I_d + \omega_s \psi_m \quad (8)$$

where $V_d$ and $V_q$ are instantaneous values of the d-axis and q-axis stator voltages; $I_d$ and $I_q$ are instantaneous values of the d-axis and q-axis stator currents; $L_d$ and $L_q$ are the d-axis and q-axis components of stator winding's inductances; $R$ is the resistance of stator winding; $\psi_m$ and $\omega_s$ are flux linkage of permanent magnet and angular frequency on stator winding, respectively.

The active power ($Ps$) and the reactive power ($Qs$) of PMG could be written as follows:

$$P_s = V_d I_d + V_q I_q \quad (9)$$

$$Q_s = V_q I_d - V_d I_q \quad (10)$$

## III. Operation of MMC

### A. Basic Principle of the MMC Operation

Basic configuration of MMC is depicted in Fig. 6. The MMC consists of three legs for each phase. The leg has two identical arms (upper and lower). Each arm consists of a number of identical sub-modules (SM) arranged in series. Each leg is also equipped with an inductor ($L_{arm}$) which it used to limit transient arm current [17]. In this paper two levels half bridge topology of sub-module is considered in which the sub-module composes of two IGBTs with anti-parallel diodes and a capacitor ($C_{SM}$). Three phase voltage of AC terminals are connected to each leg on the common point connection between upper and lower arms. In this study, AC side of MMC is connected to the stator terminal of PMG, whereas the DC side is connected to DC collection network.

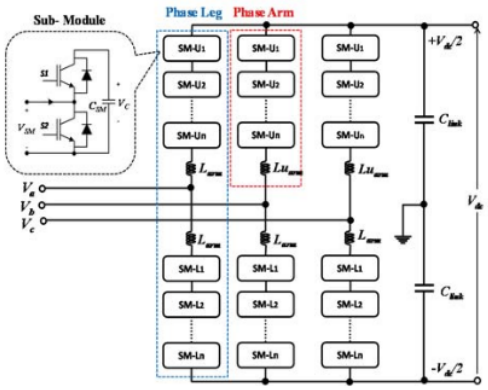


Fig. 6. MMC topology and Half Bridge Sub-Modules

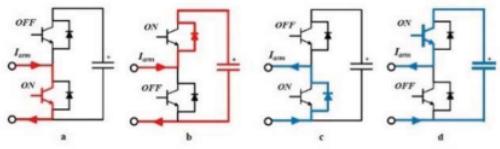


Fig. 7. Current flow in SM based on switching states

TABLE I. Switching State of SM

| Switching State | | terminal voltage of SM | Arm current Polarity | Status of Capacitor |
|---|---|---|---|---|
| S1 | S2 | | | |
| OFF | ON | 0 | + | Bypass |
| ON | OFF | $Vc$ | + | Charging |
| OFF | ON | 0 | - | Bypass |
| ON | OFF | $Vc$ | - | Discharging |

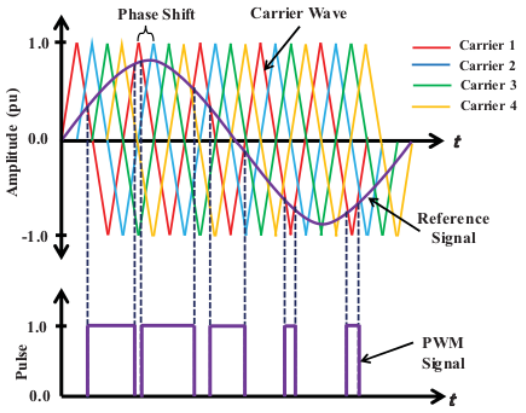


Fig. 8. Phase shift PWM technique

In operation of MMC, DC voltage ($V_{dc}$) from DC network is distributed into DC link capacitors ($C_{link}$) and then the DC voltage would be charging the entire sub-module's capacitor. Each sub-module is operated in two states, inserted and bypassed. In inserted state, switch S1 and switch S2 are respectively ON and OFF, and terminal voltage of the sub-module ($V_{SM}$) is equal to the terminal voltage of the capacitor ($V_c$). On the other hand, in bypassed state switch S1 and S2 are respectively OFF and ON, the terminal voltage of the sub-module becomes zero. The switches should be operated in complementary way to prevent short circuit of the capacitor. By organizing a number of inserted and bypassed sub-modules, the multi-step voltage output can be obtained at AC terminals of the MMC.

Fig. 7 depicts the arm current ($I_{arm}$) direction in sub-module based on switching states of S1 and S2. The red color indicates the arm current direction in the positive polarity and the blue color indicates the arm current direction in the negative polarity. Charging and discharging of sub-module's capacitor is depending on polarity of arm current. Detailed conditions of sub-module based on switching state are presented in Table I.

### B. Modulation Technique of MMC

Since the last few decade modulation and control methods for MMC have attracted attention of engineers worldwide [18]. The most commonly used modulation techniques for multilevel converter could be summarized in three categories: Multi Carrier Pulse Wave Modulation (MC-PWM), Space Vector Modulation (SVM), and Nearest Level Modulation (NLM) [19]. In this study multi carrier Phase Shifted Pulse Wave Modulation (PS-PWM) technique is considered due to its advantages. Comparing to the other approaches the phase shift PWM technique is more effective in controlling of MMC due to its superior control performance such that the power distribution between the sub-module can be provided and the voltage balance can be achieved at sub-module capacitor. Fig.

8 shows the multi carrier PS-PWM technique process. The number of carrier signal is calculated to be N-1, where N is level of the MMC (example: 7 level MMC has 6 carrier signals of modulation). The voltage and frequency of each carrier signal are equal. The phase shift ($\phi$) between the carrier signals can be calculated as $\phi = 360^o/(N-1)$ [19], hence balanced AC voltage in staircase form can be achieved at the terminal output of MMC.

## IV. Control System Of MMC Based PMG

The topology of PMG connected to 7 (seven) levels of MMC and its controller system are depicted in Fig. 9. Three phase stator winding of PMG is coupled to MMC through filter inductance ($L_{filter}$). Voltage ($V_{abc}$), current ($I_{abc}$) and rotor speed ($\omega_r$) of PMG are fed to the controller system. The controller system adjusts the three phase voltage reference ($V_{abc}$*) which is used as references signal for modulation. As stated above, in this study PS-PWM modulation is taken into account as modulation technique. MMC is configured in seven levels converter of which each phase arm consists of six sub-modules. For seven levels MMC, there are six sub-modules per arm. Therefore, there are 24 switches per phase and 72 switches in total to be controlled. The number of carrier signal is six carriers in which the phase shift of each carrier is 60°, hence it can be split as follows: $\phi_1 = 0^o \cdot \phi_2 = 60^o$, $\phi_3 = 120^o$, $\phi_4 = 180^o$, $\phi_5 = 240^o$, and $\phi_6 = 300^o$. The parameters of generator and MMC are presented in Table II.

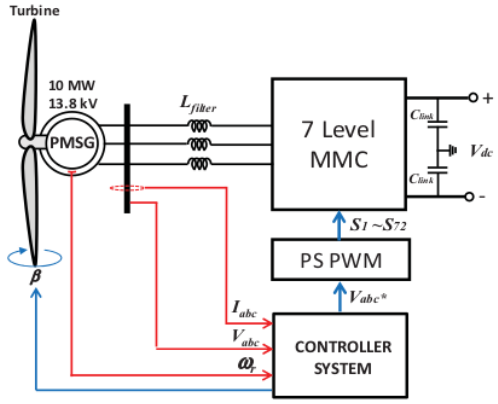


Fig. 9. Topology of PMG connected to MMC

TABLE II. PMG AND MMC PARAMETERS

| Item | Parameter | Value |
|---|---|---|
| PMG | Power Capacity | 10 MW |
| | Voltage | 13.8 kV |
| | Frequency | 20 Hz |
| | Stator Resistance | 0.02 pu |
| | Stator Leakage Reactance | 0.06 pu |
| | d-axis Reactance | 0.9 pu |
| | q_axis Reactance | 0.7 pu |
| | Magnetic Strangth | 1.4 pu |
| MMC | Number of level | 7 level |
| | AC Voltage side | 13.8 kV |
| | DC Voltage side | 30 kV |
| | Filter Inductor | 7.5 mH |
| | Arm Inductor | 0.2 mH |
| | Sub-module capacitor | 74 mF |
| | Leg Capacitor ($C_{link}$) | 50 mF |

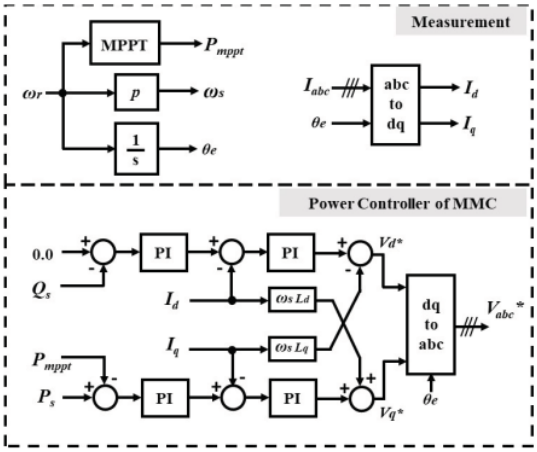


Fig. 10. MMC controller

The main purpose of the MMC system is to transfer electrical power generated by the PMG to the DC network. Fig. 10 depicts the topology of MMC controller. The MMC controller system is designed for controlling power output (active power and reactive power) from PMG. Three phase currents in sinusoidal waveform from stator winding of the generator ($I_{abc}$) is transformed into the d-axis current component ($I_d$) and the q-axis current component ($I_q$) by using Park Transformation. The power reference ($P_{mppt}$) which is calculated by MPPT (Eq.5), electrical angular speed ($\omega_s$), and rotor angle position ($\theta_e$) are obtained from rotational speed ($\omega_r$) of the generator shaft. Active power ($P_s$) and reactive power ($Q_s$) are calculated from voltage and current outputs of the generator stator winding.

In principle, the system control in MMC is same as the system control applied to general Voltage Source Converter (VSC). The active and reactive powers are controlled independently. The active power is represented by the *q*-axis component and the reactive power is represented by the *d*-axis component. Each component has two PI controllers, inner loop PI for current controller and outer loop PI for power controller. The output from inner PI controllers are reference voltages ($V_d$* and $V_q$*), and then, by using inverse Park Transformation the voltages are transformed into three phase voltage in sinusoidal form ($V_{abc}$*). Finally, $V_{abc}$* becomes the reference voltage that applied to stator winding of the generator through the MMC circuit.

## V. Simulation And Analysis

The feasibility of wind turbine direct driven PMG based MMC system which is connected to medium voltage of collection DC network is investigated through dynamic performance simulation study. The power system model depicted in Fig. 1 and the controller system model depicted in Fig. 10 have been developed into simulation in PSCAD/EMTDC platform. The simulation time step was 10 µs. The DC collection cable is represented in π model, where the parameters of the cable were 0.193 Ω/km of resistance, 0.458 mH/km of inductance and 0.085 µF/km of capacitance.

The simulation is performed in two scenarios. In the first scenario, the performance of step response of rotor speed is investigated. In the second scenario, steady state stability performance under real variable wind speed is investigated.

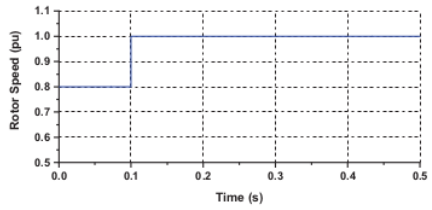


Fig. 11. Step signal input to rotor speed of PMG

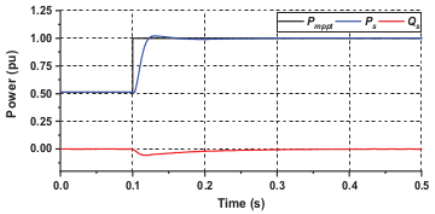


Fig. 12. Power reference and power output of PMG

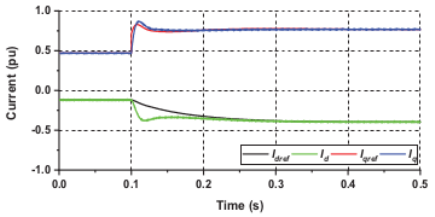


Fig. 13. The dq_axis current of stator winding of PMG

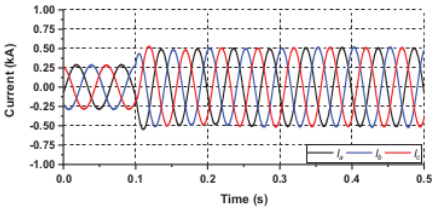


Fig. 14. Waveform current of PMG stator winding

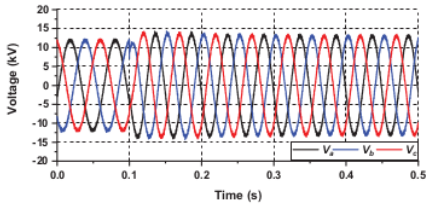


Fig. 15. Waveform voltage of PMG stator winding

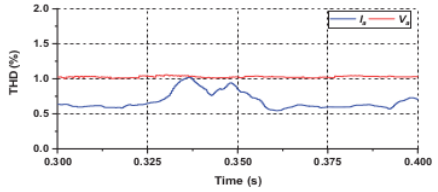


Fig. 16. Instantaneous THD of voltage and current of PMG stator winding

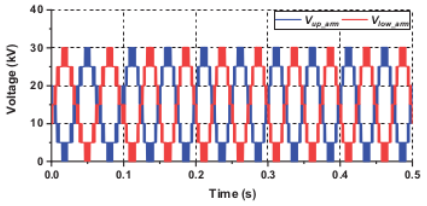


Fig. 17. Waveform of upper and lower arms voltage of MMC (phase A)

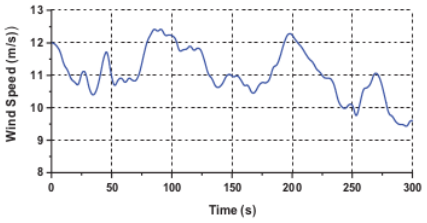


Fig. 18. Wind velocity data

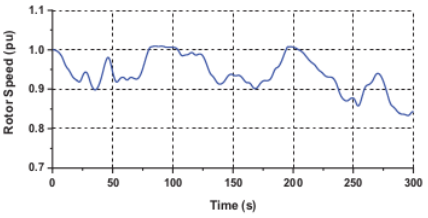


Fig. 19. Rotor speed of PMG

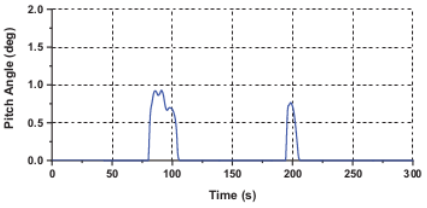


Fig. 20. Pitch angle response of the wind turbine blade

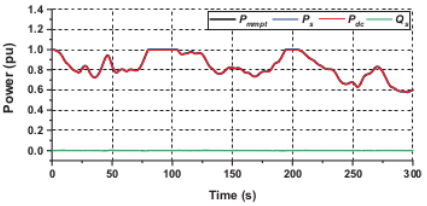


Fig. 21. Power output performance of the PMG

### *A. Step response performance analysis*

In Case 1, initial condition at $t$=0.0 s of rotor speed of PMG is 0.8 pu as shown in Fig. 11. At $t$=0.1 s the rotor speed is changed from 0.8 pu to 1.0 pu. The MPPT circuit would track the change of rotor speed in generator to obtain the power reference fed to the controller. Fig. 12 shows performance response of power output of PMG when the reference power changes. The active power can track the power reference from the MPPT very well, meanwhile the reactive power output is

kept almost constant at zero. In Fig 13, the d-axis and the q-axis currents performance inside of the controller system is presented. The d-axis current controls the reactive power and the q-axis current controls the active power of PMG. It can be confirmed that MMC based PMG system is well controllable by the proposed controller system. The waveform of current and voltage to the step disturbance can be seen respectively in Figs. 14 and 15. It can be seen that the sine waveform of the current and voltage of the PMG stator winding with small harmonic distortion can be obtained by using the MMC. The instantaneous Total Harmonic Distortion (THD) has been calculated from t = 0.3s to 0.4 s and it is seen that the THD of the waveforms is less than 1.25% as depicted in Fig 16. Finally, waveform of upper arm and lower arm voltages of MMC is shown in Fig. 17. It can be seen the voltage of both arms are complementary each other, and hence AC staircase voltage can be obtained.

### *B. Steady state performance analysis*

The steady state performance of the MMC control system is evaluated by applying real wind speed data in the simulation study. The wind velocity measured in Hokkaido, Japan is shown in Fig 18. Fig. 19 shows rotor speed of PMG under the varying wind speed. When the rotational speed exceeds the rated speed, the pitch controller changes the blades angle of attack to remain the rotor speed within 1.0 pu. Pitch angel response is shown in Fig. 20. Fig. 21 shows power output of PMG. It is seen the active power output of PMG can be controlled effectively by the MMC.

## VI. CONCLUSION

Application of Modular Multilevel Converter (MMC) to the wind turbine direct drive PMG which connected to medium voltage of DC collection network has been discussed. Dynamic performance of proposed topology and control system has been analyzed by using PSCAD/EMTDC. In step response performance analysis, the control system of MMC based PMG has well controllability to step change of rotor speed of the generator. Also, it is confirmed that the MMC in collaboration with the PMG based wind turbine can work well due to low harmonic distortion. In addition, in steady states analysis the performance of the proposed system has good stability. Finally, it can be concluded from these results the performance and thus feasibility of the proposed MMC based PMG connected to medium voltage DC collection network system are very high.

## REFERENCES


[1] International Energy Agency, "Offshor wind outlook 2019" Technology report-November 2019

[2] C. Meyer, M. Hoeing, A. Peterson, and R. W. De Doncker, "Control and design of dc grids for offshore wind farms," IEEE Transactions on Industry Applications, vol. 43, no. 6, pp. 1475–1482, 2007.

[3] J. Robinson, D. Jovcic, and G. Joos, "Analysis and design of an offshore wind farm using a mv dc grid," IEEE Transactions on Power Delivery, vol. 25, no. 4, pp. 2164–2173, 2010.

[4] J. Yang, J. Fletcher, and J. O'Reilly, "Multiterminal dc wind farm collection grid internal fault analysis and protection design," Power Delivery, IEEE Transactions on, vol. 25, no. 4, pp. 2308–2318, Oct 201

[5] S. Vogel, T.W. Rasmussen, W. Z. El-Khatib, & J. Holbøll, "DC collection network simulation for offshore wind farms," In Proceedings of EWEA Offshore 2015 Conference European Wind Energy Association (EWEA).

[6] K. Friedrich, "Modern HVDC PLUS application of VSC in modular multilevel converter topology," in: IEEE InternationalvSymposium on Industrial Electronics (ISIE), 2010.

[7] B. Jacobson, P. Karlsson, G. Asplund, L. Harnefors, T. Jonsson, "VSC-HVDC transmission with cascaded two-level converters," in: CIGRE B4-110, 2010.

[8] Y. Gangui, L. Jigang, MU Gang, Liu Yu, Liu Yang, Song Wei, "Research on modular multilevel converter suitable for direct-drive wind power system", Energy Procedia, Volume 17, Part B, pp. 1497-1506, 2012

[9] U. N. Gnanarathna, A. M. Gole, R. P. Jayasinghe, "Efficient modeling of modular multilevel HVDC converters (MMC) on electromagnetic transient simulation programs," IEEE Transactions on Power Delivery 26 (1) (2011) 316–324.

[10] S. Heier, Grid Integration of Wind Energy Conversion System, John Wiley & Sons, 1998, pp. 34-36.

[11] MATLAB documentation center [online] on http://www.mathworks.co.jp/jp/help/.

[12] S. M. Muyeen, J. Tamura, and T. Murata, Stability Augmentation of a Grid Connected Wind Farm, Green Energy and Technology, Springer-Verlag, 2009

[13] S. Achilles and M. Poller., "Direct drive synchronous machine models for stability assessment of wind farm. Available: http://www.digsilent.de/Consulting/Publications/DirectDrive_Modeling.pdf.

[14] F. M. Gonzalez-Longatt, P. Wall, V. Terzija, "A simplified model for dynamic behavior of permanent magnet synchronous generator for direct drive wind turbines", in Proc. IEEE PES PowerTech, Trondheim, Norway, 2011

[15] PSCAD/EMTDC User's Manual, Manitoba HVDC Research Center, Canada 1994.

[16] L. M. Fernandes, C. A. Garcia, F. Jurado," Operating capability as a PQ/PV node of a direct-drive wind turbine based on a permanent magnet synchronous generator," Journal of Renewable Energy, Vol. 35, pp. 1308-1318, 2010

[17] R. Marquardt, "Modular multilevel converter: an universal concept for HVDC-networks and extended DC-Busapplications," Power Electronics Conference (IPEC), 2010 International,pp. 502,507, 21-24 June 2010

[18] J. Holtz, "Pulsewidth modulation-a survey," Industrial Electronics, IEEE Transactions on , vol.39, no.5, pp.410,420, Oct 1992

[19] L.G. Franquelo; J. Rodriguez; J. I. Leon; S. Kouro; R. Portillo; M.A.M Prats, "The age of multilevel converters arrives," Industrial Electronics Magazine, IEEE , vol.2, no.2, pp.28,39, June 2008.

# Marwan2

ORIGINALITY REPORT

| 23% | 17% | 18% | 8% |
| --- | --- | --- | --- |
| SIMILARITY INDEX | INTERNET SOURCES | PUBLICATIONS | STUDENT PAPERS |

MATCH ALL SOURCES (ONLY SELECTED SOURCE PRINTED)

2%

★ Submitted to University of Pretoria

Student Paper

| | | | |
| --- | --- | --- | --- |
| Exclude quotes | On | Exclude matches | Off |
| Exclude bibliography | On | | |